Non-systematic Three-beam Effects in Dynamical Electron Diffraction and Their Use in Determination of Amplitude and Phase of Structure Factors*

K. Marthinsen,[A] *H. Matsuhata,*[B] *R. Høier*[A] *and J. Gjønnes*[B]

[A] Department of Physics and Mathematics, University of Tronheim-NTH,
7034 Trondheim, Norway.
[B] Department of Physics, University of Oslo,
Blindern, 0316 Oslo 3, Norway.

Abstract

The treatment of non-systematic multiple-beam effects in dynamical diffraction is extended. Expressions for Bloch wave degeneracies are given in the centrosymmetrical four-beam case and for some symmetrical directions. These degeneracies can be determined experimentally either as critical voltages or by locating the exact diffraction condition at a fixed voltage. The accuracy when applied to structure factor determination is comparable with the systematical critical voltage, namely 1% in U_g. The three-beam case 0, g, h is treated as well in the non-centrosymmetrical case, where it can be used for determination of phases. It is shown that the contrast features can be represented by an effective structure factor defined by the gap at the dispersion surface. From the variation in the gap with diffraction condition, a method to determine the three-phase structure invariant $\psi = \phi_g + \phi_{-h} + \phi_{h-g}$ is given. The method is based upon the contrast asymmetry in the weaker diffracted beam and can be applied in Kikuchi, convergent beam or channelling patterns. Calculations relating to channelling in backscattering are also presented.

1. Introduction

   Electron diffraction is a sensitive tool for structure studies, not only because the scattering may be recorded from very small crystal volumes. Electron scattering is sensitive to details in the average crystal structure, for example to the valence electron distribution through the form factor $(Z-F)/s^2$ and to atomic displacements because of the short wavelength. However, exploitation of these properties has so far been limited. Due to the complications arising from multiple-beam dynamical scattering, it is not straightforward to define magnitudes comparable with the integrated intensities in X-ray or neutron diffraction which can be precisely measured from the experimental pattern and interpreted directly in terms of crystal structure. An important aim in theoretical studies is therefore to establish such magnitudes, which should relate to measurable features in the diffraction pattern, also in the presence of extensive dynamical scattering.

   A set of such features, which appears in various types of diffraction patterns and in diffraction contrast, can be interpreted by two-beam-like expressions, namely

thickness fringes (Ichimiya *et al.* 1973), *s*-fringes in convergent beam discs (Goodman and Lehmpfuhl 1967), the split at Kikuchi line intersections (Gjønnes and Høier 1971) and integrated intensity across the Kikuchi line (Steeds and Vincent 1983; Taftø and Metzger 1985). These measurements can all be related to an extinction distance or gap at the dispersion surface, corresponding to an effective structure factor U^{eff}, when several interacting beams are present. Hence, they may be termed two-beam—or rather 'two Bloch wave'—features. Similar effects, including split line intersections, can be studied quantitatively in backscattering channelling patterns from bulk specimens as well (Marthinsen and Høier 1986).

A special case of such dynamical interactions occurs when U^{eff} is zero. The best known example is the systematic critical voltage (Watanabe *et al.* 1969). This is a special case of the degenerate solution in the three-beam centrosymmetrical case discussed by Gjønnes and Høier (1971) and by Hurley and Moodie (1980). In fact a wide range of degeneracies can be observed in a variety of diffraction experiments: Kikuchi patterns, convergent beam patterns and in backscattering channelling patterns. Measurement of the conditions for non-systematic degeneracies may offer a considerably extended scope for accurate determination of structure factors with electrons.
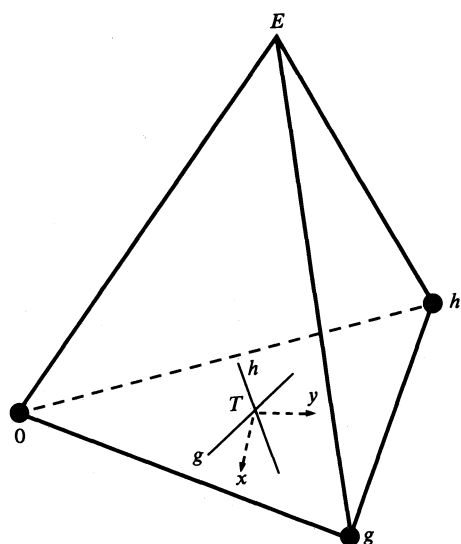

Fig. 1. Three-beam case 0, g, h, where x, y are coordinates for the projected centre of the Ewald sphere, with the exact three-beam condition $s_g = s_h = 0$ as the origin.

In the present paper the previous analytical treatment of the non-systematic three-beam case is extended in two directions: the four-beam centrosymmetrical case and the non-centrosymmetrical three-beam case. The dynamical effects in the latter case may prove to be of value in early stages of structure determination, for example, in combination with X-ray diffraction, by providing phases for a starting set in standard crystallographic programs.

2. Three- and Four-beam Centrosymmetrical Case

A general three-beam case is illustrated in Fig. 1. The diffraction condition can be described either by the projection of the centre of the Ewald sphere onto the plane of the projection or by the excitation errors $s_{g,h}$ for the two reflections g and h. Let us refer briefly to a previous treatment of the centrosymmetrical three-beam case. The three-beam eigenvalue equation for the *anpassung* γ, as derived from the matrix

$$\begin{bmatrix} -2k\gamma & U_g & U_h \\ U_g & 2ks_g-2k\gamma & U_{g-h} \\ U_h & U_{g-h} & 2ks_h-2k\gamma \end{bmatrix}, \tag{1}$$

where U_g are structure factors (in Å^{-2}), s_g excitation errors and $k = 2\pi/\lambda$ the wave number in vacuum, can be written in the form

$$(2ks_g-2k\gamma + U_g^2/2k\gamma)(2ks_h-2k\gamma + U_h^2/2k\gamma)$$

$$= (U_{g-h} + U_g U_h/2k\gamma)^2. \tag{2}$$

This is seen to represent a hyperbola in the (s_g, s_h) plane. When the right-hand side is zero, the hyperbola degenerates into two straight lines which intersect at the point

$$2ks_g = U_g(U_{g-h}/U_h - U_h/U_{g-h}), \quad 2ks_h = U_h(U_{g-h}/U_g - U_g/U_{g-h}), \tag{3}$$

which corresponds to a degenerate solution of the eigenvalue equation in the three-beam case. Experimentally this condition can be obtained by varying either the excitation errors through the diffraction condition or the primary voltage and thus the mass ratio m/m_0. In principle two excitation errors can be measured, but cases where one of them is zero may be better suited to accurate measurement—as is the case with the systematic second order critical voltage. In many interesting cases one of the structure factors involved (e.g. U_g) will be appreciably weaker than the others; then, one excitation error (s_g) will be quite small and the other (s_h) may be represented by the first term only in the expression (3), which then will correspond to the so-called Bethe potential (see e.g. Høier and Marthinsen 1983).

The three-beam expression is a useful approximation in many cases, with multiple-beam calculations reserved for refinement. In other cases four strongly excited beams may be excited and it is of interest to derive corresponding equations in this case, especially for the degeneracies. From the symmetrical matrix

$$\begin{bmatrix} -2k\gamma & U_g & U_h & U_f \\ U_g & 2ks_g-2k\gamma & U_{g-h} & U_{g-f} \\ U_h & U_{g-h} & 2ks_h-2k\gamma & U_{h-f} \\ U_f & U_{g-f} & U_{h-f} & 2ks_f-2k\gamma \end{bmatrix}, \tag{4}$$

we obtain the relation

$$(1/2k\gamma)^2 X_g X_h X_f - a^2 X_g - b^2 X_h - c^2 X_f + 2abc = 0, \tag{5}$$

where

$$X_g = -4k^2\gamma^2 + 4k^2\gamma s_g + U_g^2, \qquad X_h = -4k^2\gamma^2 + 4k^2\gamma s_h + U_h^2,$$

$$X_f = -4k^2\gamma^2 + 4k^2\gamma s_f + U_f^2, \qquad a = 2k\gamma U_{h-f} + U_h U_f,$$

$$b = 2k\gamma U_{g-f} + U_g U_f, \qquad c = 2k\gamma U_{g-h} + U_g U_h.$$

In order to compare with equation (2) we may rewrite (5) in the form

$$(X_g - b/X_f)(X_g - a/X_h) = (c - ab/X_f)^2, \tag{5a}$$

which can be regarded as the intersection with the plane $X_f = $ const. When $X_f \to \infty$, the form (2) is retrieved, i.e. $X_g X_h = c^2$. If the right-hand side is put equal to zero, we obtain again two straight lines which intersect at the point

$$X_g = bc/a, \quad X_h = ac/b, \quad X_f = ab/c, \tag{6}$$

which corresponds to a degenerate solution in the four-beam case. The three excitation errors cannot be varied independently and hence (6) must be supplemented by a relation between s_g, s_h and s_f.
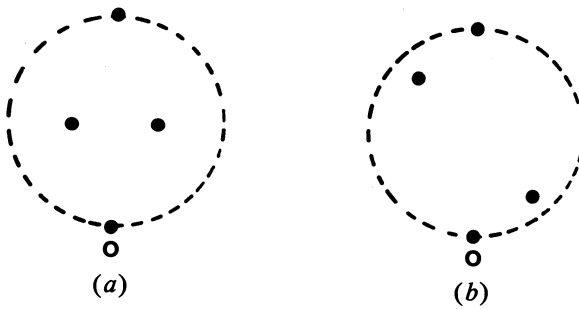

Fig. 2.   Two four-beam configurations with (*a*) symmetry $2\,mm$ and (*b*) symmetry 2.

Many cases can be evaluated by making use of symmetry. Consider the diamond shaped configuration of beams in Fig. 2*a*, which is seen to have the symmetry $2\,m$ about the centre. Along one of the mirror lines one Bloch wave solution will be antisymmetrical (m'), the remaining three will be symmetrical (m). The condition for degeneracy can be found by introducing the eigenvalue γ for the antisymmetrical Bloch wave, namely $c_0 = -c_g$, $c_h = c_f = 0$, with the eigenvalue $\gamma_3 = -U_g$, into the eigenvalue equation derived from the matrix corresponding to the symmetrical

Bloch waves, namely

$$
\begin{bmatrix}
U_g - 2k\gamma & 2\,U_h & 2\,U_h \\
2\,U_h & 2k s_h - 2k\gamma & U_{h-f} \\
2\,U_h & U_{h-f} & 2k s_f - 2k\gamma
\end{bmatrix}, \tag{7}
$$

i.e. into the eigenvalue equation

$$
(U_g - 2k\gamma)(2k s_h - 2k\gamma)(2k s_f - 2k\gamma) + 4\,U_h^2\,U_{h-f} - (U_g - 2k\gamma)\,U_{h-f}^2
$$

$$
- 2(2k s_h - 2k\gamma)\,U_h - 2(2k s_f - 2k\gamma)\,U_h^2 = 0. \tag{7a}
$$

A condition for a degenerate eigenvalue is then found by inserting $\gamma = -U_g$ in this equation:

$$
(2k s_h + U_g - U_h^2/U_g)(2k s_f + U_g - U_h^2/U_g) = (U_{f-h} - U_h^2/U_g)^2, \tag{8}
$$

which can be used to determine the position of the degeneracy across the Kikuchi line g. We may write $s_{h,f} = s(1 \pm x)$, where s is the excitation error at the symmetrical position in the centre of the four-beam configuration in Fig. 2a and x the distance from this position along the mirror line $s_g = 0$. The two positions of the degenerate points on that line are found by inserting these expressions for the excitation errors in (8):

$$
(2k s)^2 x^2 = 4k^2(s + U_g - U_{h-f})(s + U_g + U_{h-f} - 2\,U_h^2/U_g). \tag{9}
$$

The two points will merge into one degeneracy, at the symmetrical point, for a critical voltage given by

$$
2k s = 2\,U_h^2/U_g - U_g - U_{h-f}. \tag{9a}
$$

The degeneracy is observed as a vanishing contrast of the Kikuchi or Kossel line g below a non-systematic critical voltage V_c, as seen in the wide angle convergent beam patterns of $2\bar{4}2$ in ZnS reproduced in Fig. 3. A sketch of a four-beam dispersion surface along the mirror line ($s_{242} = 0$) corresponding to a situation below the critical voltage is shown in Fig. 4.

Structure factor information can be obtained from measurement either of the distance $2x$ between the two degenerate points at a given primary voltage (Fig. 3a) or of the critical voltage at which the degeneracy appears at the symmetrical position (Fig. 3b). This critical voltage was determined experimentally to 152 ± 5 kV (nominal voltage). The calculated four-beam value using Doyle and Turner (1968) atomic scattering factors for neutral atoms was 165 kV. The same value was obtained from a dynamical calculation with 100 beams which, however, may be regarded as fortuitous.
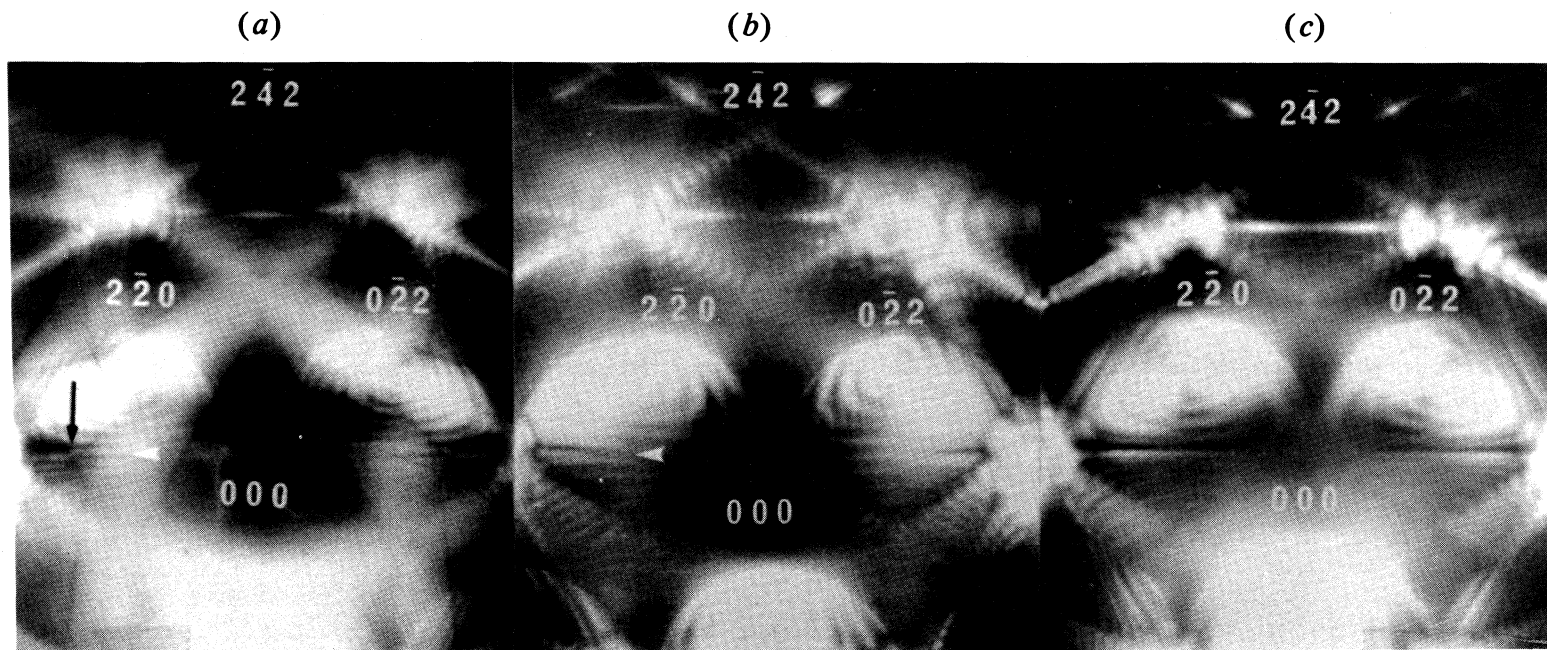
Fig. 3. Convergent beam patterns from ZnS showing extinctions appearing in the $2\bar{4}2$ reflection (*a*) below, (*b*) near and (*c*) above the critical voltage.
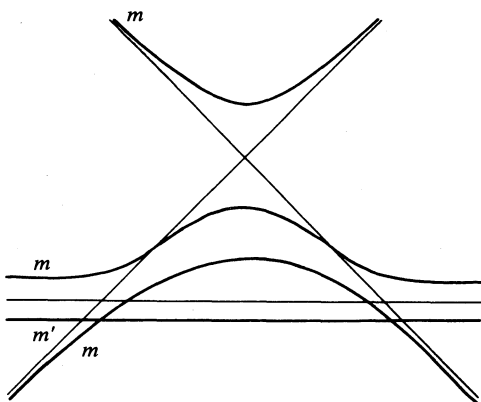
Fig. 4. Schematic of a section of the four-beam dispersion surface along the mirror line m in the configuration $2\,a$, corresponding to the lower voltage in Fig. $3\,a$.

3. Non-centrosymmetrical Case

In the non-centrosymmetrical case, the three-beam non-systematic degeneracy does not appear. The right-hand side of the three-beam equation corresponding to (2) becomes

$$(U_{g-h} + U_g\, U_h/2\,k\gamma) \times \text{complex conjugate}, \tag{10}$$

which cannot become zero for real γ. A minimum value of the gap width is obtained, however. The diffraction condition corresponding to this minimum can be used to determine a relation between structure factors, if the phase invariant is not too different from zero or π. The intensity observed at this minimum will depend upon the three-phase invariant ψ. A better option for determination of the phase invariant is offered by the variation of the gap, as seen in the contrast variation in the weaker beam with the excitation error of the coupled beam. In this case a perturbation expression based upon the Bethe approximation can be used (Høier and Marthinsen 1983):

$$|\,U_g^{\text{eff}}\,| = |\,U_g|[\{1 - |\,U_h\, U_{g-h}/\,U_h|\cos\psi/2\,k\,s_g\}^2$$

$$+ |\,U_h\, U_{g-h}/\,U_g\, 2\,k\,s_h|^2 \sin^2\psi]^{\frac{1}{2}}. \tag{11}$$

This expression for the gap, which may be generalised to include further beams, includes correction terms which are either symmetrical or antisymmetrical in s_g. It is seen that the antisymmetrical character is most pronounced at $\psi = 0$ and disappears for $\psi = \frac{1}{2}\pi$. The asymmetry of the gap, as measured by the contrast in Kikuchi or channelling pattern, is thus sensitive to the invariant phase angle ψ. Equation (11) is found to include the main features of the full dynamical calculations presented below.

We have investigated this dependence theoretically, using an example from GaP. With structure factor data as given in Table 1, the phase invariant angle is $\psi = 61°$. Calculations can be referred to Fig. 5, which shows the orientation of the coordinate axes x and y relative to the Kikuchi line positions g and h. The hyperbolic curves representing the position of the gaps at the dispersion surface are indicated; g is taken as the weaker diffracted beam.
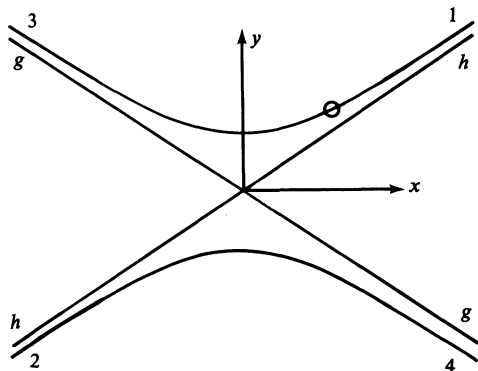
Fig. 5. Schematic representation of the position of the gap at the dispersion surface projected onto the *gh* plane. The circle indicates the position of minimum gap.

Table 1. Fourier coefficients U_g in GaP at 40 kV

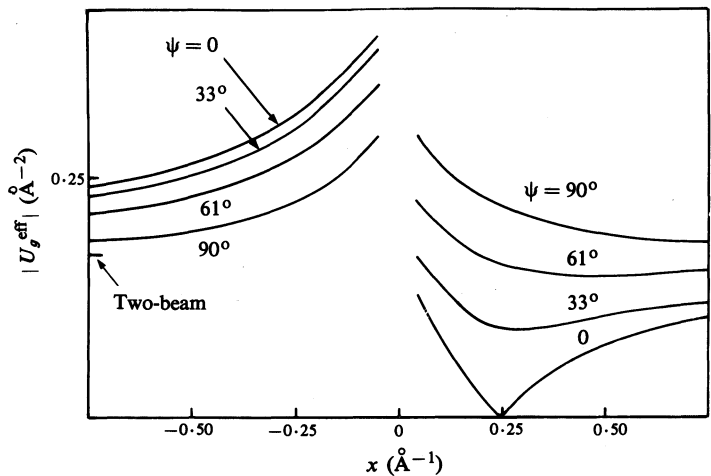| Reflection	hkl	U_{hkl} (Å^{-2})	θ_{hkl} (deg.)
g	$4\bar{4}2$	0·17	0
h	$3\bar{5}1$	0·42	−27
$h-g$	$\bar{1}\bar{1}3$	0·95	34

Fig. 6. Variation of the effective structure factor $|U_g^{\text{eff}}|$ with x for different values of the three-phase structure invariant.

For each value of x a section along the y-direction through the three-beam dispersion surface was calculated according to standard dynamical theory, using the data for GaP $3\bar{5}1$ and $4\bar{4}2$ given in Table 1. In this way the position of the gap as well as its width was determined. The effective structure factor $|U_g^{\text{eff}}|$, given by the calculated gap along the g segments of Fig. 5, is shown in Fig. 6 as function of x for four values of the phase angle ψ, keeping the amplitudes of the structure
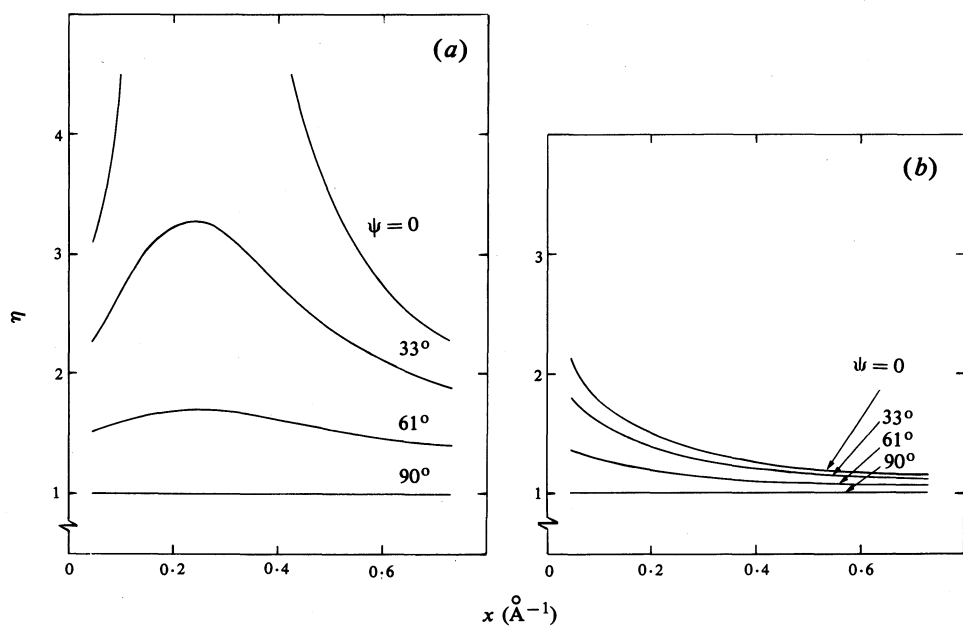
Fig. 7. Calculated asymmetry ratio η as a function of x: (*a*) the weaker beam g and (*b*) the stronger beam h.
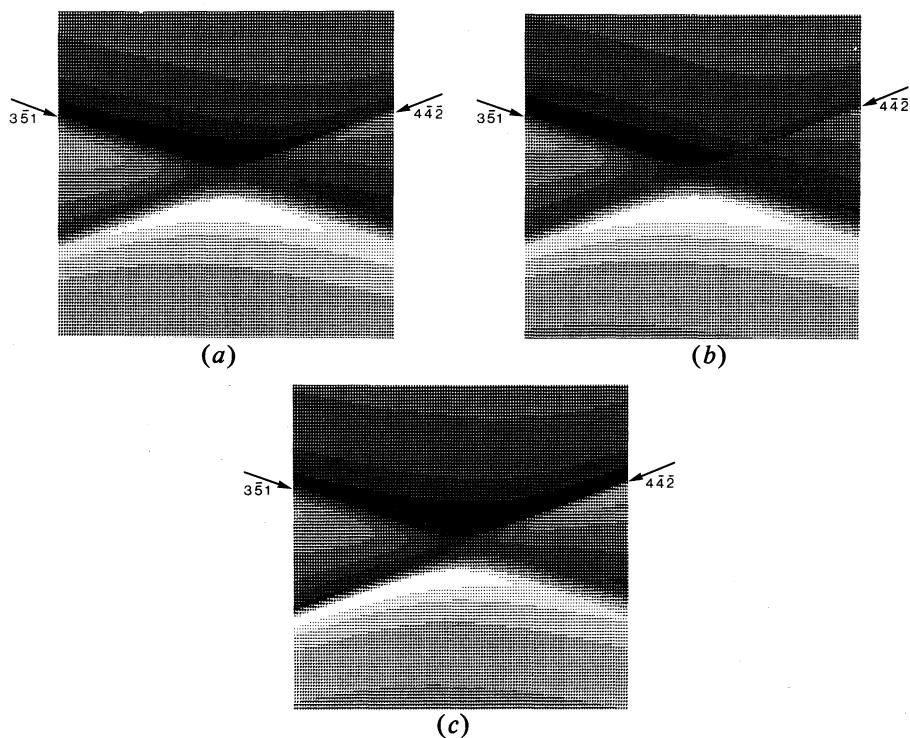

Fig. 8. Calculated channelling contrast for the $3\bar{5}1$ and $4\bar{4}\bar{2}$ three-beam case in GaP: (*a*) $\psi = 61°$, (*b*) $\psi = 0$ and (*c*) $\psi = 90°$.

factors constant. It is seen that zero gap is obtained only for the phase angle zero, i.e. the centrosymmetrical case, when the asymmetry is maximum. As the phase angle increases, the asymmetry decreases and vanishes completely at $\psi = 90°$.

Based on these results we may define an effective structure factor asymmetry ratio by the values at x and $-x$, i.e. $\eta = U_g^{\mathrm{eff}}(x) / U_g^{\mathrm{eff}}(-x)$. The variation of this ratio with x is shown in Fig. 7 for four values of the phase invariant ψ. The curves in Fig. 7*a* correspond to the weaker beam g, whereas Fig. 7*b* corresponds to the stronger h. The asymmetry effect is much less pronounced in Fig. 7*b*, as is indeed expected from equation (11). Similar curves in the X-ray case, based on intensities from the second Bethe approximation, have been given by Juretschke (1982).

The above analysis suggests that the three-phase invariant for a non-centrosymmetrical crystal may be determined by measuring this asymmetry, i.e. by comparing calculated and experimentally determined asymmetries in magnitudes reflecting the gap at the dispersion surface.

The asymmetry ratio may in principle be extracted from many types of experimental patterns, for example Kikuchi patterns, CBED patterns and backscattering channelling patterns; see the calculations reproduced in Fig. 8. Various systematic and non-systematic multiple-beam effects have recently been demonstrated in backscattering by Marthinsen and Høier (1986). The line contrast in these patterns is approximately proportional to the dispersion surface gap width, as in the Kikuchi line case. The difference between the centrosymmetrical case $\psi = 0$, the actual value $\psi = 61°$, and the value $\psi = 90°$ is clearly seen.

4. Conclusions

The three-beam effects in centrosymmetrical and non-centrosymmetrical crystals offer several magnitudes which can be measured by electron diffraction techniques and yield accurate information about amplitude and phase of structure factors. The non-systematic critical voltage effect in the centrosymmetrical case offers a considerable extension compared with the systematic case, and does not depend on instruments working in the MV range. Contrast anomalies corresponding to Bloch wave degeneracies may be measured either as critical voltages at special diffraction conditions or by measuring the position of contrast anomalies in the CBED, Kikuchi or channelling pattern for a given voltage. The accuracy of measurement may approach the systematic case.

The asymmetry effect in the general non-centrosymmetrical case can be used to determine the three-phase structure invariant ψ. Calculations of both effects can be carried out to a fair approximation using three or four beams only, in some cases by using the Bethe potential as an approximation to the effective structure factor U^{eff}. Full dynamical multiple-beam calculations can then be reserved for the refinement.

Measurement of the effects can be carried out in several diffraction experiments; convergent beam diffraction, Kikuchi patterns or channelling patterns obtained in reflection geometry. The latter type of experiment can be carried out on bulk crystals.

References

Doyle, P., and Turner, P. (1968). *Acta Cryst.* **23**, 390–7.
Gjønnes, J., and Høier, R. (1971). *Acta Cryst.* A **27**, 313–16.
Goodman, P., and Lehmpfuhl, G. (1967). *Acta Cryst.* **22**, 14–24.
Høier, K., and Marthinsen, K. (1983). *Acta Cryst.* A **39**, 854–60.
Hurley, A., and Moodie, A. F. (1980). *Acta Cryst.* A **36**, 737–8.
Ichimiya, A., Arii, T., Uyeda, R., and Fukuhara, A. (1973). *Acta Cryst.* A **29**, 724–5.
Juretschke, R. (1982). *Phys. Lett.* A **92**, 183–5.
Marthinsen, K., and Høier, R. (1986). *Acta Cryst.* A **42**, 484–92.
Steeds, J. W., and Vincent, R. (1983). *J. Microsc. Spectrosc. Electron.* **8**, 419–30.
Taftø, J., and Metzger, T. H. (1985). *J. Appl. Cryst.* **6**, 110–13.
Watanabe, D., Uyeda, R., and Fukuhara, A. (1969). *Acta Cryst.* A **24**, 138–40.